Biointerface Research in Applied Chemistry
Open-Access Journal (ISSN: 2069-5837)

Article
Volume 16, Issue 2, 2026, 58
https://doi.org/10.33263/BRIAC162.058

In-Silico Structure-Based Design of a Phytoconstituent Derived DENV2 NS5 RdRp Inhibitor

Amitesh Chakraborty [1], Santanu Giri [2], Shubhadeep Hazra [2], Aniruddha Sarkar [3], Tushar Adhikari [4,*]

[1] Department of Pharmacy, Flemming College of Pharmacy, Baruipur, Kolkata - 700144, India
[2] Department of Pharmaceutical Chemistry, DmbH Institute of Medical Science, Dadpur, Hooghly, West Bengal, India
[3] Department of Pharmacy, JIS Institute of Pharmacy, Kalyani, West Bengal 741235, India
[4] Department of Pharmaceutical Chemistry, Guru Nanak Institute of Pharmaceutical Science and Technology, Kolkata 700114, India
* Correspondence: tushar.adhikari2022@gnipst.ac.in;

Received: 15.06.2025; Accepted: 6.11.2025; Published: 15.04.2026

Abstract: Dengue fever, an *Aedes* mosquito-borne disease caused by the Dengue virus (DENV), currently lacks an FDA-approved drug. One key enzyme involved in dengue virus replication is the NS5 RNA-dependent RNA polymerase (RdRp) protein. This research focuses on identifying and designing a novel inhibitor of NS5 RdRp (PDB ID: 6IZY) of DENV2 through the screening of phytoconstituents using *in-silico* approaches. The compound 2-allyl-1-amino-7,7-dimethyltetradecahydro-5H-pyrrolo[2',1':2,3]pyrimido[6,1-a]isoquinoline-3,8,9-triol was designed and found to exhibit favorable docking interactions at the palm domain of RdRp. The compound demonstrated high predicted safety (LD_{50} = 3500 mg/kg), a wide therapeutic index, and no blood–brain barrier permeability. These computational findings suggest its potential as a lead molecule; however, further validation through molecular dynamics and *in vitro* assays is necessary to confirm its inhibitory efficacy.

Keywords: Dengue; DENV NS5 RdRp; molecular docking; novel compound; pharmacophore; QSAR.

1. Introduction

Dengue fever is a growing global concern and poses a challenge, especially in tropical countries like India [1]. This has caused serious concerns in over 120 countries [2]. According to current WHO statistics, approximately 400 million people are infected with Dengue fever annually, of whom approximately one-fourth develop the illness [3]. Aedes aegypti and Aedes albopictus mosquitoes are the primary vectors for this disease. Dengue virus (DENV1–4) has four serotypes. It belongs to the order Flavivirales, family Flaviviridae, and genus Flavivirus. Since it is an arthropod-borne virus (Arbovirus), it acts as the main causative agent of dengue [4,5]. Clinical manifestations of dengue mainly include flu-like symptoms. In severe cases, it may progress to dengue hemorrhagic fever (DHF) or dengue shock syndrome (DSS), which are the primary causes of fatality [6]. Traditional vaccination has shown limited efficacy against the Dengue virus, and currently, no recognized drug therapies are available for its treatment [7–9]. In this context, there is a growing interest in identifying novel drug candidates.

Dengue has a complex pathogenesis that primarily involves hepatocytes. The DENV particles are released into the host's bloodstream through the bite of an infected mosquito, which then targets the immune system. The virus then enters the cell via clathrin-mediated endocytosis. The endosome has an acidic microenvironment, which induces conformational changes in the viral envelope, leading to viral membrane fusion and the release of the nucleocapsid into the host cytoplasm. Host and viral proteases then cleave it into structural proteins (capsid C, membrane M, and envelope E) and non-structural proteins (NS1, NS2A, NS2B, NS3, NS4A, NS4B, and NS5) [10,11].

Non-structural proteins represent specific drug targets for dengue treatment. NS3 protease/helicase, along with its cofactor NS2B, is essential for polyprotein processing. NS5 methyltransferase (MTase) catalyzes the 5′ capping of viral RNA [12–14]. The DENV NS5 protein also possesses RNA-dependent RNA polymerase (RdRp) activity, which plays a crucial role in RNA capping and polymerization during viral replication [15–17].

The high specificity of the NS5 RdRp protein in targeting DENV makes it one of the most important molecular targets for controlling dengue infection [17,18]. Recent advancements in protein analysis and analytical techniques have enabled the elucidation of its crystal structure by X-ray crystallography and NMR [19]. Currently, there are very few drugs that specifically target DENV NS5 RdRp, and the Food and Drug Administration has approved no dedicated drug. It was seen that some drugs that were repurposed show efficacy in inhibiting RdRp but have multiple toxicities and complications, as shown in Table 1.

Table 1. Drug candidates that might have RdRp inhibition action

Sl. No.	PubChem ID	Compound name	Limitations as a drug candidate for DENV	References	Software used
1.	2732	Chlorthalidone	Officially used as a thiazide diuretic and repurposed for DENV with a therapeutic index of 5000mg/kg LD_{50}, but shows nephrotoxicity and immunotoxicity, BBB penetration, Cytochrome CYP2C9 inhibition, and blood pressure fluctuation.	[20,21]	ProTox 3.0
2.	119607	Valdecoxib	Used as a COX-2 inhibitor with an LD_{50} of about 6081mg/kg. But has carcinogenic properties, with the ability to penetrate the BBB. It is banned in India and the US.	[20,22–24]	ProTox 3.0; ADMETlab 3.0
3.	11691726	Balapiravir	High toxicity like liver, neuro, nephron, respiratory toxicity; carcinogenic, mutagenic. The therapeutic window is narrow with LD_{50} 826mg/kg. Penetrate the BBB. Shows very little efficacy for DENV treatment. Issues of hematology, like neutropenia and lymphopenia	[25,26]	ProTox 3.0

Based on ethnomedical practices and evidence, plants such as papaya, neem, tulsi, betel, pomegranate, amla, and pineapple are considered potential remedies for the treatment of dengue fever. The therapeutic effects, particularly of papaya leaf extracts, are attributed to their bioactive phytoconstituents [27–32]. Various synthetic and repurposed inhibitors have been evaluated against the DENV NS5 RdRp; most exhibit limited efficacy, poor specificity, or undesirable toxicity, and no FDA-approved drug currently exists (Table 1). To address and bridge this gap, the present study integrates *in silico computational approaches, including QSAR-based pharmacophore modeling, to design a novel NS5 RdRp inhibitor from natural compounds* to develop potential dengue therapeutics.

2. Materials and Methods

2.1. Literature review.

Several folklore and ethnomedicinal reports describe the use of various plant parts, including stems, bark, leaves, roots, and fruits, for the treatment of dengue fever. Decoctions or extracts of these plant parts are widely used to reduce symptoms. Around 40 published articles from journals such as Elsevier, Springer, Wiley, and Taylor and Francis, indexed in Scopus and Web of Science, were screened to substantiate the evidence for natural remedies for dengue fever. Eighteen relevant articles were finally selected to collect information on the plant parts commonly used. For each plant, the major phytoconstituents were obtained from the "Indian Medicinal Plants, Phytochemistry and Therapeutics 2.0 (IMPPAT 2.0) Database" (https://cb.imsc.res.in/imppat/). A total of 100 phytoconstituents were selected for further analysis.

2.2. Protein selection and validation.

Different protein structures available in the Protein Data Bank were screened for the NS5 RdRp of the DENV2 virus. The protein (PDB ID: 6IZY) was selected due to its high resolution (2.11 Å) and absence of mutations. It was elucidated by X-ray diffraction and validated using a Ramachandran plot generated in BIOVIA Discovery Studio 2025 Client.

The protein structure was refined in UCSF Chimera 1.17.3 by removing ligands and heteroatoms and adding hydrogens and charges.

Internal validation was performed by docking the co-crystallized ligand using AutoDock4 (v4.2.6).

2.3. Drug likeness screening and molecular docking.

Among the 100 selected phytoconstituents, 3D conformer structures were downloaded from PubChem (https://pubchem.ncbi.nlm.nih.gov/) in .sdf format. SMILES strings of these molecules were analyzed for Lipinski's rule of five compliance using SwissADME (http://www.swissadme.ch/). Molecules violating more than two Lipinski rules were discarded. In cases of single violations, additional filters such as Veber's and Ghose criteria were applied to ensure acceptable drug-likeness using SwissADME. Molecules showing low gastrointestinal absorption were also excluded from further analysis.

The selected ligands were docked against the prepared 6IZY protein using AutoDock4 (v4.2.6). Docking parameters were as follows: Grid box dimensions: 77.0923 Å (X), 71.6470 Å (Y), 61.1339 Å (Z); Grid spacing: 0.375 Å; Number of GA runs: 100; Exhaustiveness: 8.

Binding energy, RMSD, and minimized energy values were recorded. Standard reference ligands (as listed in Table 1) were also docked to enable comparative evaluation of docking scores.

2.4. Pharmacophore generation and QSAR analysis.

Based on docking scores, the ligands were ranked from highest to lowest and grouped into five clusters (each containing approximately 12 compounds). Common structural and electronic features across groups were used to generate pharmacophores. The five pharmacophores were then combined to develop a comprehensive consensus pharmacophore model. Pharmacophore models were generated from the top-scoring ligands using LigandScout

4.4, Discovery Studio 2025 Client, and Pharmit to ensure cross-platform validation of pharmacophoric features.

The pharmacophore model showed three modifiable regions (R1, R2, and R3) that consistently interacted with key residues of the NS5 RdRp active site (PDB ID: 6IZY). These sites were chosen because they represented the chemical positions influencing hydrogen bonding, hydrophobic contact, and steric compatibility within the palm and finger domains of the enzyme, thus offering maximum scope for structure–activity optimization.

A quantitative structure activity relationship (QSAR) model was developed using PaDEL-Descriptor (v2.21) for molecular descriptor generation, KNIME (v4.8) for data preprocessing, and QSARINS (v2.2.4) for model construction and validation. Docking scores and selected topological, electronic, and hydrophobic descriptors were analyzed using multiple linear regression (MLR) and partial least squares (PLS). Feature selection via a genetic algorithm improved model robustness. The model exhibited strong statistical reliability (R^2 = 0.87, Q^2 = 0.79, R^2_{pred} = 0.81) and complied with OECD QSAR validation criteria.

The validated model was employed to generate analogs by substituting various functional groups at the R1–R3 positions, followed by molecular docking and ADMET screening. SwissADME and ADMETlab 3.0 were used for ADME profiling, and ProTox-III predicted toxicity. The final optimized ligand, with the best docking score, a high LD_{50}, favorable pharmacokinetics, and no predicted blood–brain barrier permeability, was identified as the lead compound.

3. Results and Discussion

Dengue fever remains a significant public health challenge, especially in tropical regions, with no FDA-approved antiviral drug available [16,19]. The viral NS5 RNA-dependent RNA polymerase (RdRp) is crucial for RNA replication and capping, making it a key molecular target for antiviral development.

3.1. Selection of ethnomedicinally important plants and ligands.

A total of 57 phytoconstituents from ten ethnomedicinal plants traditionally used in dengue management were screened. Following drug-likeness filtering via SwissADME, ligands with high gastrointestinal absorption and less than two Lipinski violations were retained. Table 2, shown below, illustrates the different traditionally important plants that have shown a beneficial role in treating dengue fever. The most unique phytoconstituent present in each plant has also been listed in Table 2, along with its PubChem ID.

3.2. Protein selection and validation.

The DENV2 NS5 RdRp crystal structure (PDB ID: 6IZY) was validated through a Ramachandran plot, showing 92.4% residues in favored regions, confirming acceptable stereochemical quality (Figure 1). No ligand was pre-bound, ensuring unbiased active-site docking. The protein showed no mutations and did not contain any pre-attached ligand to its crystal structure, but the active sites have already been identified.

Table 2. Literature review of different plant parts used as remedies for dengue fever, as per folklore and ethnomedicine.

Sl. No.	Botanical name	Family	Common name	Part(s) used	Biological role/ MOA in dengue treatment	Unique phyto-components	PubChem Compound ID (CID)	Form used	Ref.
1	*Adhatoda vasica* Nees	Acanthaceae	Malabar nut	Leaves	Treat thrombo-cytopenia; Mucolytic effect	7-Methoxyvasicinone Adhatodine Anisotine Deoxyvasicinone Eicosane Fenretinide Tritriacontane Vasicine Vasicinol Vasicinone	101995828 5316460 442884 68261 8222 5288209 12411 667496 442934 442935	Leaf juice	[33]
2	*Amaranthus spinosus* L.	Amaran-thaceae	Amaranth	Leaves	Inhibits mast cell-mediated anaphylactic reactions	Alpha-Spinasterol Amaranthine Betacyanins Betalains Hentriacontane Isoquercetin Quercetin Nicotinic acid Stearic acid Trigonelline	5281331 6325284 112500418 56841626 12410 5280804 5280343 938 5281 5570	Leaf juice; Decoction	[34,35]
3	*Ananas comosus* (L.) Merr.	Brome-liaceae	Pineapple	Fruit	Anti-edematous; decreases bradykinin and thromboxane A2 levels	4-Carvomenthenol Antheraxanthin Astaxanthin Bromelain Furaneol gamma-Butyrolactone gamma-Eudesmol Pectin Pipecolic acid	11230 5281223 5281224 44263865 19309 7302 6432005 3722617 849	Fruit (ripe) juice	[36,37]
4	*Azadirachta indica* A. Juss.	Meliaceae	Neem	Leaves	Inhibition of viral envelope protein;	Azadirachtanin Azadirachtin delta-Elemene	102146586 5281303 12309449	Raw leaves decoction	[38,39]

Sl. No.	Botanical name	Family	Common name	Part(s) used	Biological role/ MOA in dengue treatment	Unique phyto-components	PubChem Compound ID (CID)	Form used	Ref.
					Stimulates Th1 cytokine response	gamma-Muurolene Germacrene B Nicotiflorin Nimbinene Nimbocinolide Vilasinin	12313020 5281519 5318767 44715635 13875774 85729		
5	*Carica papaya* L.	Caricaceae	Papaya	Leaves, fruit	Increased platelet and WBC count; increased CCL2 and MCP-1 levels in plasma	2-Methoxy-4-vinylphenol Benzyl isothiocyanate Carpaine, Eucalyptol Farnesol Humulene Neophytadiene Nonanal Phytofluene Salidroside	332 2346 442630 2758 3327 5281520 10446 31289 6436722 159278	Leaf juice/ extract; Unripe fruit	[40–44]
6	*Euphorbia hirta* L.	Euphor-biaceae	Asthma Plant	Whole plant	Interfere with NS5 RNA polymerase; Balances Th1/Th2 response; Increase platelet count	Afzelin Cerotate Cycloartenol Euphorbin, Euphorbol hexacosanoate Glyoxylic acid Quercitol, Taraxerol Tinyatoxin Triacontanoic acid	5316673 5461023 92110 16197487 101280172 760 441437 92097 76972186 10471	Aerial part decoction; Oral decoction and infusion	[45]
7	*Ocimum tenuiflorum* L.	Lamiaceae	Tulsi	Leaves	Antiviral, immunostimulant; interfering with the envelope protein	alpha-Bisabolene beta-Vetivenene Cyclosativene Eugenol Isolongifolene Maalialcohol Rosmarinic acid Spathulenol	86597 14475467 519960 3314 11127402 10944069 5281792 92231	Leaf juice	[46]

Sl. No.	Botanical name	Family	Common name	Part(s) used	Biological role/ MOA in dengue treatment	Unique phyto-components	PubChem Compound ID (CID)	Form used	Ref.
						Ursolic acid Verbenone	64945 29025		
8	*Psidium guajava L.*	Myrtaceae	Guava	Leaves; Young fruit	Manage thrombocytopenia, increase megakaryocyte differentiation	(+)-delta-Cadinene (+)-gamma-Gurjunene Aromadendrene beta-Farnesene Guajavin A Levomenol Psidinin A Psidinin B Psiguavin T-Muurolol	441005 90805 11095734 5281517 131752682 442343 131752720 131752719 131752694 3084331	Leaf decoction; Fruit extract	[47]
9	*Piper betle* L.	Piperaceae	Paan leaves	Leaves	Stimulates thrombopoiesis; inhibits viral attachment and replication	1-Triacontanol 2-Undecanone Allylpyrocatechol Apiole beta-Guaiene Bicyclogermacrene Chavibetol Guaiazulene Myrtenol Safrole Viridiflorene	68972 8163 292101 10659 6949 13894537 596375 3515 10582 5144 10910653	Leaf extract; juice	[48,49]
10	*Punica granatum* L.	Lythraceae	Pome-granate	Fruit	Improves RBC regeneration post-hemorrhage	Brevifolin Copaene Ellagic acid Flavylium Granatin A Maslinic acid Punicalagin Punicalin Punicic acid Valencene	66654 12303902 5281855 145858 131752596 73659 16129719 92131301 5281126 9855795	Fruit juice	[50-52]

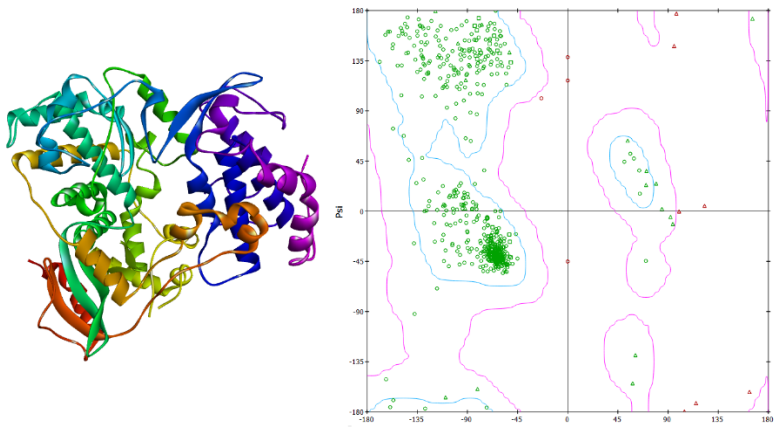

Figure 1. The 3D structure of protein 6IZY (left) and Ramachandran plot (right).

Based on screening of ligands by Lipinski rule violations and further Veber's and Ghose criteria, the following ligands were initially discarded: Amaranthine, Betacyanins, Betalains, Granatin A, Nicotiflorin, Psidinin A, Psidinin B, Psiguavin, Punicalagin, Punicalin, Punicic acid, Isoquercetin, Adhatodine, Azadirachtin, Nimbinene, Pectin, Phytofluene, Bromelain, Euphorbin, Guajavin A. Other ligands that were found to have very poor GI absorption were also rejected from the list.

3.3. Molecular docking analysis.

Docking studies using AutoDock 4.2 revealed that several compounds exhibited notable affinity for the NS5 RdRp active pocket, as shown in Table 3. Standard ligands selected were also docked.

Table 3. Molecular docking analysis for different naturally occurring bioactive compounds against Dengue Virus RdRp (6IZY).

Sl. No	Protein PDB ID	Ligand PubChem CID	Compound name	Minimized energy (kcal/mol)	Binding affinity (kcal/mol)	Compound designation
0.	6IZY	2732	Chlorthalidone	984.13	-7.2	A
0.	6IZY	119607	Valdecoxib	650.45	-7.0	B
0.	6IZY	11691726	Balapiravir	420.34	-7.0	C
1	6IZY	92110	Cycloartenol	2128.4	-8.7	1A
2	6IZY	64945	Ursolic acid	805.65	-8.5	1B
3	6IZY	145858	Flavylium	178.56	-8.5	1C
4	6IZY	442630	Carpaine	332.5	-8.5	1D
5	6IZY	73659	Maslinic acid	837.07	-8.5	1E
6	6IZY	5281331	Alpha-Spinasterol	569.98	-8.4	1F
7	6IZY	9855795	Valencene	180.75	-8.3	1G
8	6IZY	92097	Taraxerol	851.8	-8.2	1H
9	6IZY	76972186	Tinyatoxin	952.39	-8.2	1I
10	6IZY	5280343	Quercetin	380.43	-8.1	1J
11	6IZY	5281792	Rosmarinic acid	209.67	-8.1	1K
12	6IZY	3515	Guaiazulene	369.95	-8	1L
13	6IZY	5281223	Antheraxanthin	2122.76	-8	2A
14	6IZY	5288209	Fenretinide	595.76	-8	2B
15	6IZY	92231	Spathulenol	1727.92	-7.7	2C
16	6IZY	442884	Anisotine	430.11	-7.6	2D
17	6IZY	5281855	Ellagic acid	227.58	-7.6	2E
18	6IZY	11095734	Aromadendrene	1698.37	-7.5	2F
19	6IZY	6949	beta-Guaiene	293	-7.4	2G
20	6IZY	6432005	gamma-Eudesmol	264.33	-7.4	2H
21	6IZY	90805	(+)-gamma-Gurjunene	315.96	-7.3	2I
22	6IZY	11127402	Isolongifolene	457.88	-7.2	2J
23	6IZY	12313020	gamma-Muurolene	173.65	-7.2	2K

Sl. No	Protein PDB ID	Ligand PubChem CID	Compound name	Minimized energy (kcal/mol)	Binding affinity (kcal/mol)	Compound designation
24	6IZY	3084331	T-Muurolol	212.79	-7.2	2L
25	6IZY	10944069	Maalialcohol	1710.14	-7.2	3A
26	6IZY	441005	(+)-delta-Cadinene	241.83	-7.1	3B
27	6IZY	5316673	Afzelin	581.17	-7.1	3C
28	6IZY	10910653	Viridiflorene	1641.02	-7	3D
29	6IZY	159278	Salidroside	296.38	-6.6	3E
30	6IZY	442935	Vasicinone	288.7	-6.6	3F
31	6IZY	667496	Vasicine	267.25	-6.6	3G
32	6IZY	68261	Deoxyvasicinone	262.29	-6.4	3H
33	6IZY	12309449	delta-Elemene	218.48	-6.3	3I
34	6IZY	3327	Farnesol	148.85	-6.3	3J
35	6IZY	442343	Levomenol	218.81	-6.3	3K
36	6IZY	442934	Vasicinol	263.58	-6.1	3L
37	6IZY	5144	Safrole	244.83	-6.1	4A
38	6IZY	11230	4-Carvomenthenol	155.64	-5.9	4B
39	6IZY	3314	Eugenol	169.59	-5.9	4C
40	6IZY	10582	Myrtenol	649.92	-5.8	4D
41	6IZY	292101	Allylpyrocatechol	95.27	-5.8	4E
42	6IZY	596375	Chavibetol	105.19	-5.8	4F
43	6IZY	29025	Verbenone	648.9	-5.6	4G
44	6IZY	10659	Apiole	310.5	-5.6	4H
45	6IZY	332	2-Methoxy-4-vinylphenol	99.78	-5.6	4I
46	6IZY	2758	Eucalyptol	344.57	-5.4	4J
47	6IZY	66654	Brevifolin	330.12	-5.4	4K
48	6IZY	2346	Benzyl isothiocyanate	79.77	-5.3	5A
49	6IZY	5570	Trigonelline	67.47	-5.1	5B
50	6IZY	441437	Quercitol	153.37	-5	5C
51	6IZY	849	Pipecolic acid	61.42	-4.9	5D
52	6IZY	938	Nicotinic acid	58.73	-4.8	5E
53	6IZY	19309	Furaneol	152.29	-4.6	5F
54	6IZY	31289	Nonanal	30.59	-4.5	5G
55	6IZY	8163	2-Undecanone	35.97	-4.5	5H
56	6IZY	7302	gamma-Butyrolactone	151.57	-3.8	5I
57	6IZY	760	Glyoxylic acid	5.07	-3.6	5J

The Sl. No. 0 indicates three standard drugs often used for the inhibition of the RdRp of Dengue Virus.

3.4. Pharmacophore generation.

Each pharmacophore developing software identified a common three-point pharmacophore model comprising two hydrogen-bond donors, one hydrogen-bond acceptor, and a hydrophobic centroid corresponding to critical interactions within the palm domain of NS5 RdRp (PDB ID: 6IZY). The final pharmacophore that was built is shown in Figure 2.

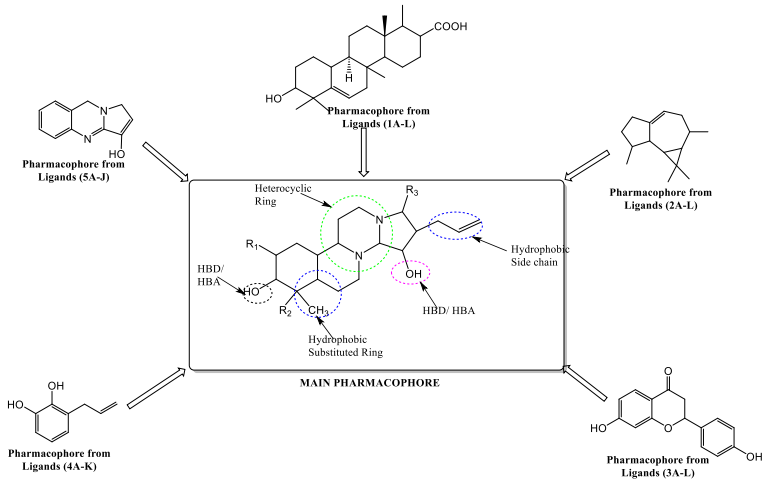

Figure 2. Pharmacophore designing based on different groups of molecular docking analysis.

Table 4. QSAR Modelling of the designed pharmacophore with different functional groups.

Sl. No	Compound designation	Functional group			Binding energy (kcal/mol)	Toxicity scale	LD_{50} value (mg/kg)	MW (g/mol)	Hepatotoxicity	Neurotoxicity	Nephrotoxicity	Respiratory toxicity	Mutagenicity	Carcinogenicity
		R1	R2	R3										
1.	IA	H	H	H	-5.4	4	2000	318.49	0.72	0.54	0.73	-0.81	0.72	0.76
2.	IB	CH_3	H	H	-6.6	4	2000	332.52	0.75	0.57	0.73	-0.69	0.73	0..71
3.	IC	NH_2	H	H	-6.5	5	5000	333.51	0.79	0.54	0.71	-0.82	0.67	0.62
4.	**ID**	**OH**	**H**	**H**	**-6.7**	**5**	**5000**	**334.49**	**0.78**	**0.84**	**0.62**	**-0.69**	**0.63**	**0.63**
5.	IE	$COCH_3$	H	H	-6.4	5	5000	360.53	0.66	0.78	0.56	-0.73	0.67	0.63
6.	IF	Cl	H	H	-6.0	5	5000	352.94	0.70	0.55	0.66	-0.68	0.63	0.68
7.	IG	F	H	H	-6.0	5	5000	338.48	0.70	0.57	0.67	-0.68	0.66	0.65
8.	**IIA**	**OH**	**CH_3**	**H**	**-6.7**	**5**	**3500**	**348.52**	**0.86**	**0.52**	**0.62**	**-0.90**	**0.60**	**0.59**
9.	IIB	OH	NH_2	H	-6.0	5	3500	349.51	0.82	0.72	0.64	-0.82	0.68	0.67
10.	IIC	OH	OH	H	-6.5	5	3500	350.49	0.86	0.92	0.62	-0.84	0.65	0.69
11.	IID	OH	$COCH_3$	H	-6.4	5	5000	376.53	0.79	0.90	0.63	-0.85	0.64	0.63
12.	IIE	OH	C_2H_5	H	-6.6	5	5000	362.55	0.79	0.83	0.72	-0.84	0.73	0.64
13.	IIIA	OH	CH_3	NO_2	-6.1	5	3500	395.49	0.71	0.74	0.51	-0.84	0.51	0.58
14.	**IIIB**	**OH**	**CH_3**	**NH_2**	**-6.6**	**5**	**3500**	**365.51**	**0.79**	**0.50**	**0.56**	**-0.90**	**0.67**	**0.53**
15.	IIIC	OH	CH_3	CH_3	-6.0	5	3500	364.52	0.84	0.53	0.59	-0.90	0.73	0.53
16.	IIID	OH	CH_3	$COCH_3$	-6.8	4	1375	392.53	0.82	0.52	0.53	-0.89	0.73	0.50
17.	IIIE	OH	CH_3	OH	-6.5	3	366.5	500	0.75	-0.56	0.54	-0.87	0.71	0.58
18.	IIIF	OH	CH_3	$CONH_2$	-7.1	4	2000	393.52	0.72	-0.57	0.51	-0.92	0.71	0.57
19.	IIIG	OH	CH_3	COOH	-6.8	4	1375	394.51	0.84	-0.50	-0.52	-0.90	0.67	0.50

The values indicate the probability of activity (active/ inactive). A negative sign before the predicted values indicates that the compound shows toxicity. Absence of '-' sign before the values indicates the software-based analysis shows no toxicity.

3.5. Pharmacophore modeling by QSAR.

In QSAR analysis, for different groups (R1, R2, and R3), specific functional groups were selected based on the docking scores the compound showed with each functional group, followed by ADMET analysis. For each substituted molecule, the details of its molecular docking and ADMET are shown in Table 4. The individual molecules so analyzed are shown in Figure 3.

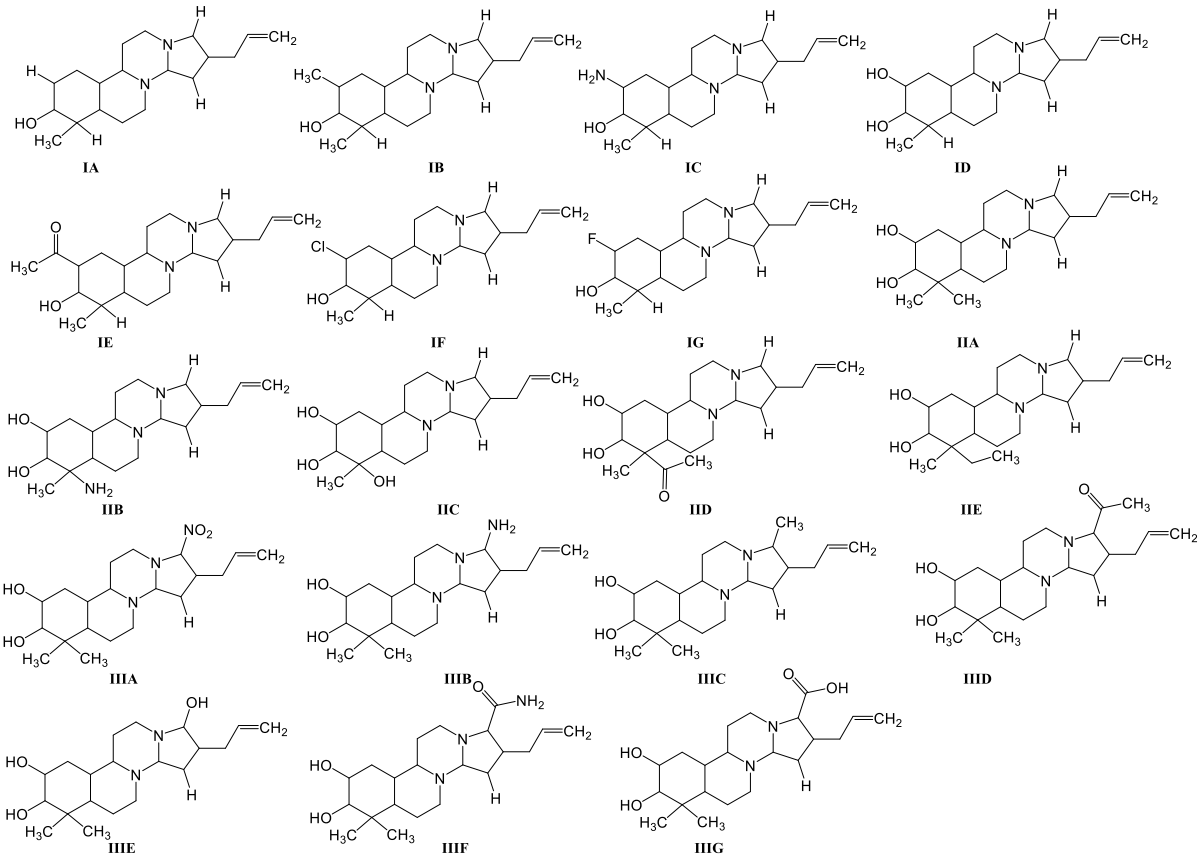

Figure 3. Different designed compounds for QSAR Analysis. Compound ID was selected for R_1, IIA for R_2. The final molecule predicted was Compound IIIB.

For the R1 position, a hydroxyl group (−OH) was selected as shown in the compound ID. This was because all other substituents showed a higher probability of active toxicities. Moreover, the docking score of −OH at R1 with the receptor was also found to be the highest.

Similarly, for the R2 position, after fixing −OH at R1, it was found that the $-CH_3$ or methyl group proved to be the best fit. However, it was found that this compound could penetrate the blood–brain barrier (BBB), which might lead to central nervous system–related side effects.

To overcome this limitation, different substituents were tested at the R3 position while keeping the hydroxyl and methyl groups at R1 and R2, respectively, fixed. The amino group ($-NH_2$) was identified as the most promising substituent (Compound IIIB). Although it showed a slightly higher docking score than the carboxyl and acetyl groups, it was favored due to its superior ADMET properties. Quantitative validation supported the selection of Compound IIIB as the final lead molecule. It demonstrated stable hydrogen-bond interactions with key residues Glu501 (2.18 Å), Lys525 (2.93 Å), and Ser656 (2.45 Å) within the palm domain of NS5 RdRp, indicating a robust binding profile. *In-silico* ADMET analysis showed that it was the only substituent that prevented BBB permeability and exhibited minimal predicted organ toxicities

except for mild respiratory toxicity. It was predicted to have the highest LD_{50} value of 3500mg/kg, which is considered to be much safer and belongs to class 5 of toxicity as per ProTox software. Thus, it had a wide therapeutic window.

3.6. Final molecule prediction and ADMET analysis.

The final molecule, thus predicted, is named 2-allyl-1-amino-7,7-dimethyltetradecahydro-5H-pyrrolo[2',1':2,3]pyrimido[6,1-a]isoquinoline-3,8,9-triol as shown in Figure 4.

SMILES: OC1C(O)C(C)(C)C(CCN2C3CCN4C2C(O)C(CC=C)C4N)C3C1

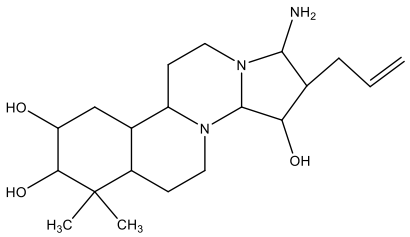

Figure 4. Final compound designed by QSAR analysis.

The physicochemical properties of this molecule are mentioned in Table 5.

Table 5. Physicochemical properties of the predicted molecules.

Physicochemical parameters	Properties	Details	Software/ website used for prediction
Drug likeliness (Lipinski Rule)	Mol. Wt.	365.51 g/mol	SwissADME
	Rotatable bonds	2	
	H-bond acceptors	6	
	H-bond donors	4	
	iLOGP	2.77	
	Molar Refractivity	108.88	
Solubility	Class	Soluble	SwissADME
	Log S	-2.68	
Pharmacokinetic parameters	GI Absorption	High	SwissADME
	BBB permeability	No	
	Inhibitor of metabolism (CYP1A2, CYP2C19; CYP2C9, CYP2D6 and CYP3A4)	No	
	Clearance (CL)	8 mL/min/kg (moderate)	ADMETlab 3.0
	LD_{50}	3500 mg/kg	ProTox 3.0
Toxicity	Tox21-stress response pathways	Inactive	ProTox 3.0
	Molecular Initiating Events	Inactive	
	Toxicity Scale	5	

The binding interactions of the standard and predicted compounds are shown in Figure 5.

It was found that the standard drugs for Dengue NS5 RdRp protein, such as Chlorthalidone and Balapiravir, showed docking scores of −7.2 kcal/mol and −7.0 kcal/mol, respectively. These values are comparable to the predicted drug substance, which exhibited a binding energy of −6.7 kcal/mol and was found to be bound at the active site of the enzyme. This close similarity in binding affinity further supports the efficacy and potential potency of the predicted compound. Quantitative validation through comparative docking energy and interaction analysis indicates that the predicted molecule shows comparable binding interactions and distances within the palm sub-domain, similar to the reference inhibitors, thereby strengthening its reliability as a potential RdRp inhibitor.

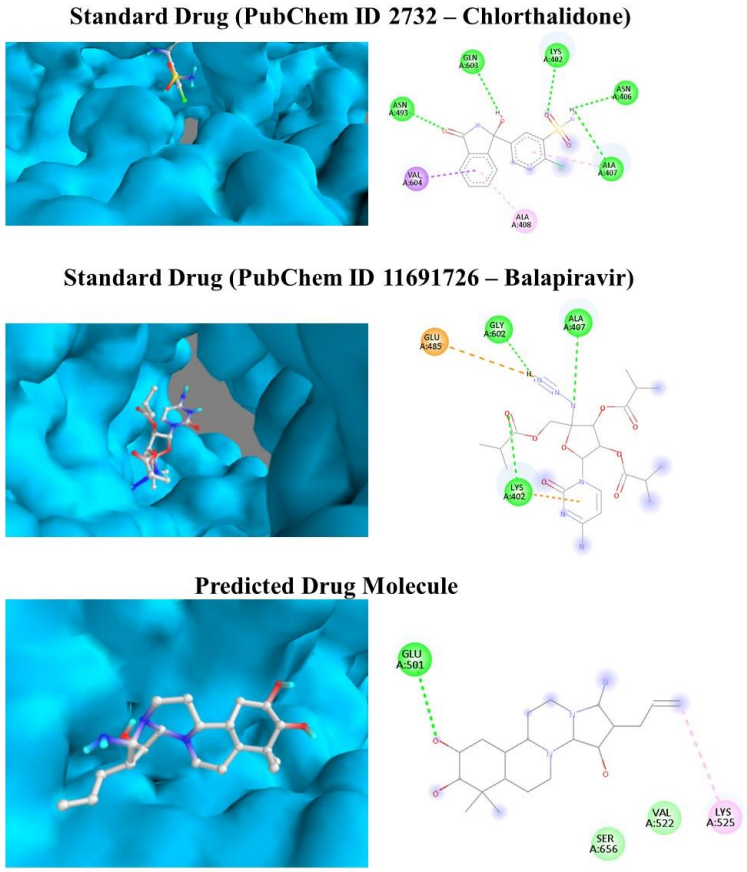

Figure 5. Molecular docking in the binding cavity (left) and 2D molecular interaction (right) of standard ligands of RdRp (6IZY) and the predicted compound.

3.7. Molecular mechanism of predicted drug molecule.

To show *in vivo* actions, the molecular mechanism of the drug should be predicted. Among the different non-structural proteins found in the DENV2 virus, NS5 is the largest [53]. The N-terminal consists of a Methyltransferase (MTase) responsible for methylation at the 5′ RNA cap [54]. On the other hand, the RdRp domain at the C-terminal is responsible for RNA replication and forms positive-sense and negative-sense RNA strands. For proper functioning, NS5 RdRp requires Mn^{2+} or Mg^{2+} as cofactors [55,56].

This NS5 RdRp protein contains three subdomains, namely the Palm subdomain (residues 497–542 and 601–705), which is the catalytically active and structurally conserved site; the Thumb domain or RNA-binding domain with two conserved motifs (706–900 amino acid residues); third is the Finger domain, which is the mobile domain and responsible for chnages in conformation (residues 273-314, 416-496 and 543-600) [53].

The predicted molecule is capable of forming multiple interactions (both bonded and non-bonded) with the different residues of amino acids of RdRp protein, especially at Glutamic acid 501, Serine 656, Valine 522, and Lysine 525. The binding domains indicate that the molecule binds at the palm subdomain and inhibits the enzyme's active site [56]. It was seen that the hydroxyl group of the predicted molecule forms a bond with Glutamic acid 501. This residue is crucial for metal binding. Interaction of the molecule with this domain might disrupt the metal coordination sphere and prevent the binding of magnesium and manganese ions to the active site, which would render the enzyme inactive. The terminal methylene group of the molecule interacts with Lysine 525, displacing lysine from nucleoside triphosphate poisoning

and hindering the enzyme's stable confirmation [56]. The entire mechanism of the predicted novel drug molecule is hypothesized in Figure 6.

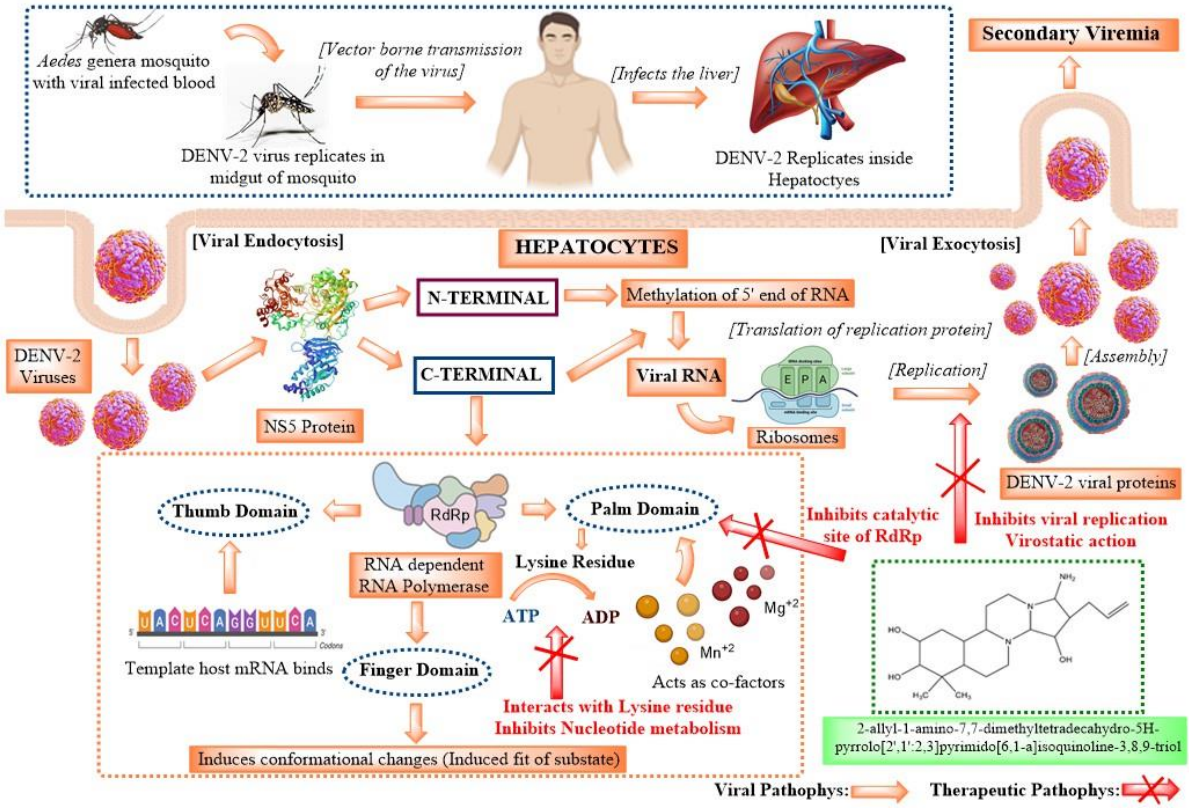

Figure 6. Mechanism of action of the predicted drug molecule as a virustatic.

The cumulative effect of these interactions between the structural features of the predicted molecule and the amino acid residues of the Palm domain of the RdRp protein renders the RdRp protein non-functional, thereby preventing viral RNA replication in the host cell and preventing the progression of viral infection. These putative evidences from *in-silico* computational studies predicts that the drug molecule is virustatic and not virucidal.

Since the drug candidate has a lower toxicity profile, better clearance, and a very good metabolic profile, it can be further advanced for synthesis and *in vitro* antiviral analysis by predicting its IC_{50} value.

4. Conclusions

Dengue Hemorrhagic Fever and Dengue Shock Syndrome are two major clinical manifestations of dengue fever, both associated with high fatality rates. Currently, dengue fever treatment consists only of adjuvant therapies, with no specific targeted drug. Based on ethnomedicinally important plant products, computational analysis and *in-silico* ADMET profiling were performed to develop a pharmacophore. This was followed by the prediction of a novel molecule using QSAR analysis, capable of binding to and antagonizing the NS5 RdRp protein of DENV2, thereby halting viral replication within the host cell. The predicted molecule based on computational analysis, identified as 2-allyl-1-amino-7,7-dimethyltetradecahydro-5H-pyrrolo[2′,1′:2,3]pyrimido[6,1-a]isoquinoline-3,8,9-triol, was predicted to be safe based on computational toxicity models, with an LD_{50} of 3500 mg/kg. It exhibited a satisfactory ADMET profile and did not penetrate the blood–brain barrier (BBB). Further analysis of this molecule using QM/MM and molecular dynamics methods should be conducted. This research presented

only predictive computational analysis and should be followed by synthesis and in vitro antiviral evaluation to ensure the efficacy of this molecule.

Author Contributions

Conceptualization, A.C.; methodology, A.C.; software, A.C.; validation, A.C.; formal analysis, A.C.; investigation, A.C.; resources, A.C.; data curation, A.C.; writing—original draft preparation, A.C.; writing—review and editing, A.C.; visualization, A.C. All authors have read and agreed to the published version of the manuscript.

Institutional Review Board Statement

Not applicable.

Informed Consent Statement

Not applicable.

Data Availability Statement

Data supporting the findings of this study are available upon reasonable request from the corresponding author.

Funding

This research received no external funding.

Acknowledgments

The authors acknowledge their respective institutions for giving them the opportunity to conduct the research.

Conflicts of Interest

The authors declare no conflict of interest.

Abbreviations

The following abbreviations are used in this manuscript:

Abbreviation	Full Form
DENV	Dengue Virus
RdRp	RNA-dependent RNA Polymerase
NS	Non-Structural (e.g., NS5 = Non-Structural protein 5)
DHF	Dengue Hemorrhagic Fever
DSS	Dengue Shock Syndrome
FDA	Food and Drug Administration
WHO	World Health Organization
MOA	Mechanism of Action
ADME	Absorption, Distribution, Metabolism, Excretion
ADMET	Absorption, Distribution, Metabolism, Excretion, and Toxicity
QSAR	Quantitative Structure–Activity Relationship
GI	Gastrointestinal
BBB	Blood–Brain Barrier

Abbreviation	Full Form
LD50	Median Lethal Dose
SMILES	Simplified Molecular Input Line Entry System
PDB	Protein Data Bank
SDF	Structure Data file format
MW	Molecular Weight
CYP	Cytochrome P450 enzyme (e.g., CYP2C9, CYP3A4)
H-bond	Hydrogen Bond
iLOGP	Individual Log Partition Coefficient (Log Po/w)
R1, R2, R3	Substitution sites on the predicted molecule
RMSD	Root Mean Square Deviation
2D/3D	Two-Dimensional / Three-Dimensional
IMMPAT	Indian Medicinal Plants, Phytochemistry, And Therapeutics
XRD	X-ray Diffraction
QM/MM	Quantum Mechanics/Molecular Mechanics
IC50	Half maximal inhibitory concentration
LogS	Logarithm of Solubility

References

1. Khan, M.B.; Yang, Z.-S.; Lin, C.-Y.; Hsu, M.-C.; Urbina, A.N.; Assavalapsakul, W.; Wang, W.-H.; Chen, Y.-H.; Wang, S.-F. Dengue overview: An updated systemic review. *J. Infect. Public Health* **2023**, *16*, 1625-1642, https://doi.org/10.1016/j.jiph.2023.08.001.
2. Kularatne, S.A.; Dalugama, C. Dengue infection: Global importance, immunopathology and management. *Clin. Med.* **2022**, *22*, 9-13, https://doi.org/10.7861/clinmed.2021-0791.
3. Roy, S.K.; Bhattacharjee, S. Dengue virus: epidemiology, biology, and disease aetiology. *Can. J. Microbiol.* **2021**, *67*, 687-702, https://doi.org/10.1139/cjm-2020-0572.
4. Sukhralia, S.; Verma, M.; Gopirajan, S.; Dhanaraj, P.S.; Lal, R.; Mehla, N.; Kant, C.R. From dengue to Zika: the wide spread of mosquito-borne arboviruses. *Eur. J. Clin. Microbiol. Infect. Dis.* **2019**, *38*, 3-14, https://doi.org/10.1007/s10096-018-3375-7.
5. eClinicalMedicine. Dengue as a growing global health concern. *eClinicalMedicine* **2024**, *77*, 102975, https://doi.org/10.1016/j.eclinm.2024.102975.
6. Chawla, P.; Yadav, A.; Chawla, V. Clinical implications and treatment of dengue. *Asian Pac. J. Trop. Med.* **2014**, *7*, 169-178, https://doi.org/10.1016/S1995-7645(14)60016-X.
7. Obi, J.O.; Gutiérrez-Barbosa, H.; Chua, J.V.; Deredge, D.J. Current Trends and Limitations in Dengue Antiviral Research. *Trop. Med. Infect. Dis.* **2021**, *6*, 180, https://doi.org/10.3390/tropicalmed6040180.
8. Tayal, A.; Kabra, S.K.; Lodha, R. Management of Dengue: An Updated Review. *Indian J. Pediatr.* **2023**, *90*, 168-177, https://doi.org/10.1007/s12098-022-04394-8.
9. Jasamai, M.; Yap, W.B.; Sakulpanich, A.; Jaleel, A. Current prevention and potential treatment options for dengue infection. *J. Pharm. Pharm. Sci.* **2019**, *22*, 440-456, https://doi.org/10.18433/jpps30216.
10. Sinha, S.; Singh, K.; Ravi Kumar, Y.S.; Roy, R.; Phadnis, S.; Meena, V.; Bhattacharyya, S.; Verma, B. Dengue virus pathogenesis and host molecular machineries. *J. Biomed. Sci.* **2024**, *31*, 43, https://doi.org/10.1186/s12929-024-01030-9.
11. Bhatt, P.; Sabeena, S.P.; Varma, M.; Arunkumar, G. Current Understanding of the Pathogenesis of Dengue Virus Infection. *Curr. Microbiol.* **2021**, *78*, 17-32, https://doi.org/10.1007/s00284-020-02284-w.
12. Muhammad, A.; Shehryar, H.; Abbas, H.; Khalid Mohammed, K. Development in the Inhibition of Dengue Proteases as Drug Targets. *Curr. Med. Chem.* **2024**, *31*, 2195-2233, https://doi.org/10.2174/0929867331666230918110144.
13. Benmansour, F.; Trist, I.; Coutard, B.; Decroly, E.; Querat, G.; Brancale, A.; Barral, K. Discovery of novel dengue virus NS5 methyltransferase non-nucleoside inhibitors by fragment-based drug design. *Eur. J. Med. Chem.* **2017**, *125*, 865-880, https://doi.org/10.1016/j.ejmech.2016.10.007.
14. Benarroch, D.; Egloff, M.-P.; Mulard, L.; Guerreiro, C.; Romette, J.-L.; Canard, B. A Structural Basis for the Inhibition of the NS5 Dengue Virus mRNA 2′-*O*-Methyltransferase Domain by Ribavirin 5′-Triphosphate*. *J. Biol. Chem.* **2004**, *279*, 35638-35643, https://doi.org/10.1074/jbc.M400460200.

15. Nascimento, I.J.d.S.; Santos-Júnior, P.F.d.S.; Aquino, T.M.d.; Araújo-Júnior, J.X.d.; Silva-Júnior, E.F.d. Insights on Dengue and Zika NS5 RNA-dependent RNA polymerase (RdRp) inhibitors. *Eur. J. Med. Chem.* **2021**, *224*, 113698, https://doi.org/10.1016/j.ejmech.2021.113698.
16. Shimizu, H.; Saito, A.; Mikuni, J.; Nakayama, E.E.; Koyama, H.; Honma, T.; Shirouzu, M.; Sekine, S.-i.; Shioda, T. Discovery of a small molecule inhibitor targeting dengue virus NS5 RNA-dependent RNA polymerase. *PLoS Negl. Trop. Dis.* **2019**, *13*, e0007894, https://doi.org/10.1371/journal.pntd.0007894.
17. Klema, V.J.; Ye, M.; Hindupur, A.; Teramoto, T.; Gottipati, K.; Padmanabhan, R.; Choi, K.H. Dengue Virus Nonstructural Protein 5 (NS5) Assembles into a Dimer with a Unique Methyltransferase and Polymerase Interface. *PLOS Pathogens* **2016**, *12*, e1005451, https://doi.org/10.1371/journal.ppat.1005451.
18. Benmansour, F.; Eydoux, C.; Querat, G.; de Lamballerie, X.; Canard, B.; Alvarez, K.; Guillemot, J.-C.; Barral, K. Novel 2-phenyl-5-[(E)-2-(thiophen-2-yl)ethenyl]-1,3,4-oxadiazole and 3-phenyl-5-[(E)-2-(thiophen-2-yl)ethenyl]-1,2,4-oxadiazole derivatives as dengue virus inhibitors targeting NS5 polymerase. *Eur. J. Med. Chem.* **2016**, *109*, 146-156, https://doi.org/10.1016/j.ejmech.2015.12.046.
19. Low, J.G.H.; Ooi, E.E.; Vasudevan, S.G. Current Status of Dengue Therapeutics Research and Development. *J. Infect. Dis.* **2017**, *215*, S96-S102, https://doi.org/10.1093/infdis/jiw423.
20. Ahmadi, K.; Jahantigh, H.R.; Ahmadi, N.; Shahbazi, B. Repurposing FDA-approved drugs and natural compounds to inhibit the RNA-dependent RNA polymerase domain of dengue virus 2 or dengue virus 3. *Sci. Rep.* **2025**, *15*, 12698, https://doi.org/10.1038/s41598-025-96284-0.
21. Agarwal, R.; Sinha, A.D.; Tu, W. Mechanisms of Antihypertensive Effect of Chlorthalidone in Advanced Chronic Kidney Disease: A Causal Mediation Analysis. *Clin. J. Am. Soc. Nephrol.* **2024**, *19*, 1025-1032, https://doi.org/10.2215/CJN.0000000000000484.
22. Chavez, M.L.; DeKorte, C.J. Valdecoxib: A review. *Clinical Therapeutics* **2003**, *25*, 817-851, https://doi.org/10.1016/S0149-2918(03)80110-8.
23. Nussmeier Nancy, A.; Whelton Andrew, A.; Brown Mark, T.; Langford Richard, M.; Hoeft, A.; Parlow Joel, L.; Boyce Steven, W.; Verburg Kenneth, M. Complications of the COX-2 Inhibitors Parecoxib and Valdecoxib after Cardiac Surgery. *N. Engl. J. Med.* **2005**, *352*, 1081-1091, https://doi.org/10.1056/NEJMoa050330.
24. Atukorala, I.; Hunter, D.J. Valdecoxib: the rise and fall of a COX-2 inhibitor. *Expert Opin. Pharmacother.* **2013**, *14*, 1077-1086, https://doi.org/10.1517/14656566.2013.783568.
25. Chen, Y.-L.; Abdul Ghafar, N.; Karuna, R.; Fu, Y.; Lim Siew, P.; Schul, W.; Gu, F.; Herve, M.; Yokohama, F.; Wang, G.; Cerny, D.; Fink, K.; Blasco, F.; Shi, P.-Y. Activation of Peripheral Blood Mononuclear Cells by Dengue Virus Infection Depotentiates Balapiravir. *J. Virol.* **2014**, *88*, 1740-1747, https://doi.org/10.1128/JVI.02841-13.
26. Nguyen, N.M.; Tran, C.N.B.; Phung, L.K.; Duong, K.T.H.; Huynh, H.l.A.; Farrar, J.; Nguyen, Q.T.H.; Tran, H.T.; Nguyen, C.V.V.; Merson, L.; Hoang, L.T.; Hibberd, M.L.; Aw, P.P.K.; Wilm, A.; Nagarajan, N.; Nguyen, D.T.; Pham, M.P.; Nguyen, T.T.; Javanbakht, H.; Klumpp, K.; Hammond, J.; Petric, R.; Wolbers, M.; Nguyen, C.T.; Simmons, C.P. A Randomized, Double-Blind Placebo Controlled Trial of Balapiravir, a Polymerase Inhibitor, in Adult Dengue Patients. *J. Infect. Dis.* **2013**, *207*, 1442-1450, https://doi.org/10.1093/infdis/jis470.
27. Lim, S.P. Dengue drug discovery: Progress, challenges and outlook. *Antiviral Res.* **2019**, *163*, 156-178, https://doi.org/10.1016/j.antiviral.2018.12.016.
28. Rehman, B.; Ahmed, A.; Khan, S.; Saleem, N.; Naseer, F.; Ahmad, S. Exploring plant-based dengue therapeutics: from laboratory to clinic. *Trop. Dis. Travel Med. Vaccines.* **2024**, *10*, 23, https://doi.org/10.1186/s40794-024-00232-1.
29. Altamish, M.; Khan, M.; Baig, M.S.; Pathak, B.; Rani, V.; Akhtar, J.; Khan, A.A.; Ahmad, S.; Krishnan, A. Therapeutic Potential of Medicinal Plants against Dengue Infection: A Mechanistic Viewpoint. *ACS Omega* **2022**, *7*, 24048-24065, https://doi.org/10.1021/acsomega.2c00625.
30. Abd Kadir, S.L.; Yaakob, H.; Mohamed Zulkifli, R. Potential anti-dengue medicinal plants: a review. *J. Nat. Med.* **2013**, *67*, 677-689, https://doi.org/10.1007/s11418-013-0767-y.
31. Alagarasu, K.; Patil, P.; Kaushik, M.; Chowdhury, D.; Joshi, R.K.; Hegde, H.V.; Kakade, M.B.; Hoti, S.L.; Cherian, S.; Parashar, D. *In Vitro* Antiviral Activity of Potential Medicinal Plant Extracts Against Dengue and Chikungunya Viruses. *Front. Cell. Infect. Microbiol.* **2022**, *12*, 866452, https://doi.org/10.3389/fcimb.2022.866452.

32. Hasani, S.J.; Sgroi, G., Esmaeilnejad, B.; Nofouzi, K.; Mahmoudi, S.S.; Shams, N.; Samiei, A.; Khademi, P. Recent advances in the control of dengue fever using herbal and synthetic drugs. *Heliyon*. **2025,** *11(3)*, e41939, https://doi.org/10.1016/j.heliyon.2025.e41939
33. Pugazhenthan, T.; Gopinathan, N.; Vijayakumar Arumugam, R.; Meenalochini Prakash, G.; Sree Sudha Tanguturi, Y.; Sajitha, V.; Eswaran, t. Molecular Docking Analysis of *Adhatoda vasica* with Thromboxane A_2 Receptor (TXA_2R) (6IIU) and Antiviral Molecules for Possible Dengue Complications. *Infect. Disord. Drug Targets* **2023**, *23*, e180722206836, https://doi.org/10.2174/1871526522666220718101544.
34. Patil, S.D.; Patel, M.R.; Patel, S.R.; Surana, S.J. *Amaranthus spinosus* Linn. inhibits mast cell-mediated anaphylactic reactions. *J. Immunotoxicol.* **2012**, *9*, 77-84, https://doi.org/10.3109/1547691X.2011.631609.
35. Baraniak, J.; Kania-Dobrowolska, M. The Dual Nature of Amaranth—Functional Food and Potential Medicine. *Foods* **2022**, *11*, 618, https://doi.org/10.3390/foods11040618.
36. Calderón-Arguedas, O.; Troyo, A.; Moreira-Soto, R.D.; Marín, R.; Taylor, L. Dengue viruses in *Aedes albopictus* Skuse from a pineapple plantation in Costa Rica. *J. Vector Ecol.* **2015**, *40*, 184-186, https://doi.org/10.1111/jvec.12149.
37. Kumar, V.; Garg, V.; Dureja, H. Therapeutic Application of Pineapple: A Review. *Recent Adv. Food Nutr. Agric.* **2023**, *14*, 107-125, https://doi.org/10.2174/2772574X14666230522114039.
38. Parida, M.M.; Upadhyay, C.; Pandya, G.; Jana, A.M. Inhibitory potential of neem (Azadirachta indica Juss) leaves on Dengue virus type-2 replication. *J. Ethnopharmacol.* **2002**, *79*, 273-278, https://doi.org/10.1016/S0378-8741(01)00395-6.
39. Singh, P.K.; Rawat, P. Evolving herbal formulations in management of dengue fever. *J. Ayurveda Integr. Med.* **2017**, *8*, 207-210, https://doi.org/10.1016/j.jaim.2017.06.005.
40. Sathyapalan, D.T.; Padmanabhan, A.; Moni, M.; P-Prabhu, B.; Prasanna, P.; Balachandran, S.; Trikkur, S.P.; Jose, S.; Edathadathil, F.; Anilkumar, J.O.; Jayaprasad, R.; Koramparambil, G.; Kamath, R.C.; Menon, V.; Menon, V. Efficacy & safety of *Carica papaya* leaf extract (CPLE) in severe thrombocytopenia (≤30,000/µl) in adult dengue – Results of a pilot study. *PLOS ONE* **2020**, *15*, e0228699, https://doi.org/10.1371/journal.pone.0228699.
41. Norahmad, N.A.; Mohd Abd Razak, M.R.; Mohmad Misnan, N.; Md Jelas, N.H.; Sastu, U.R.; Muhammad, A.; Ho, T.C.D.; Jusoh, B.; Zolkifli, N.A.; Thayan, R.; Mat Ripen, A.; Zainol, M.; Syed Mohamed, A.F. Effect of freeze-dried Carica papaya leaf juice on inflammatory cytokines production during dengue virus infection in AG129 mice. *BMC Complement. Altern. Med.* **2019**, *19*, 44, https://doi.org/10.1186/s12906-019-2438-3.
42. Subenthiran, S.; Choon, T.C.; Cheong, K.C.; Thayan, R.; Teck, M.B.; Muniandy, P.K.; Afzan, A.; Abdullah, N.R.; Ismail, Z. *Carica papaya* Leaves Juice Significantly Accelerates the Rate of Increase in Platelet Count among Patients with Dengue Fever and Dengue Haemorrhagic Fever. *Evid. Based Complement. Alternat. Med.* **2013**, *2013*, 616737, https://doi.org/10.1155/2013/616737.
43. Ahmad, N.; Fazal, H.; Ayaz, M.; Abbasi, B.H.; Mohammad, I.; Fazal, L. Dengue fever treatment with *Carica papaya* leaves extracts. *Asian Pac. J. Trop. Biomed.* **2011**, *1*, 330-333, https://doi.org/10.1016/S2221-1691(11)60055-5.
44. Sathasivam, K.; Ramanathan, S.; Mansor, S.M.; Haris, M.R.M.H.; Wernsdorfer, W.H. Thrombocyte counts in mice after the administration of papaya leaf suspension. *Wien. Klin. Wochenschr.* **2009**, *121*, 19-22, https://doi.org/10.1007/s00508-009-1229-0.
45. Perera, S.D.; Jayawardena, U.A.; Jayasinghe, C.D. Potential Use of Euphorbia hirta for Dengue: A Systematic Review of Scientific Evidence. *J. Trop. Med.* **2018**, *2018*, 2048530, https://doi.org/10.1155/2018/2048530.
46. Kaushik, S.; Kaushik, S.; Dar, L.; Yadav, J.P. Eugenol isolated from supercritical fluid extract of Ocimum sanctum: a potent inhibitor of DENV-2. *AMB Express* **2023**, *13*, 105, https://doi.org/10.1186/s13568-023-01607-x.
47. Batoro, J.; Siswanto, D. Ethnomedicinal survey of plants used by local society in Poncokusumo district, Malang, East Java Province, Indonesia. *Asian J. Med. Biol. Res.* **2017**, *3*, 158-167.
48. Martianasari, R.; Hamid, P.H. Larvicidal, adulticidal, and oviposition-deterrent activity of Piper betle L. essential oil to Aedes aegypti. *Vet. World* **2019**, *12*, 367-371, https://doi.org/10.14202/vetworld.2019.367-371.
49. Biswas, P.; Anand, U.; Saha, S.C.; Kant, N.; Mishra, T.; Masih, H.; Bar, A.; Pandey, D.K.; Jha, Niraj K.; Majumder, M.; Das, N.; Gadekar, Vijaykumar S.; Shekhawat, M.S.; Kumar, M.; Radha; Proćków, J.; Lastra, J.M.P.d.l.; Dey, A. Betelvine (*Piper betle* L.): A comprehensive insight into its ethnopharmacology, phytochemistry, and pharmacological, biomedical and therapeutic attributes. *J. Cell. Mol. Med.* **2022**, *26*, 3083-3119, https://doi.org/10.1111/jcmm.17323.

50. Salles, T.S.; Meneses, M.D.F.; Caldas, L.A.; Sá-Guimarães, T.E.; de Oliveira, D.M.; Ventura, J.A.; Azevedo, R.C.; Kuster, R.M.; Soares, M.R.; Ferreira, D.F. Virucidal and antiviral activities of pomegranate (*Punica granatum*) extract against the mosquito-borne Mayaro virus. *Parasites Vectors* **2021**, *14*, 443, https://doi.org/10.1186/s13071-021-04955-4.
51. Ismat, F.; Tariq, A.; Shaheen, A.; Ullah, R.; Raheem, K.; Muddassar, M.; Mahboob, S.; Abbas, W.; Iqbal, M.; Rahman, M. Inhibition of NS2B-NS3 protease from all four serotypes of dengue virus by punicalagin, punicalin and ellagic acid identified from *Punica granatum*. *J. Biomol. Struct. Dyn.* **2025**, *43*, 7604-7619, https://doi.org/10.1080/07391102.2024.2314258.
52. Chavda, V.P.; Kumar, A.; Banerjee, R.; Das, N. Ayurvedic and Other Herbal Remedies for Dengue: An Update. *Clin. Complement. Med. Pharmacol.* **2022**, *2*, 100024, https://doi.org/10.1016/j.ccmp.2022.100024.
53. Yap Thai, L.; Xu, T.; Chen, Y.-L.; Malet, H.; Egloff, M.-P.; Canard, B.; Vasudevan Subhash, G.; Lescar, J. Crystal Structure of the Dengue Virus RNA-Dependent RNA Polymerase Catalytic Domain at 1.85-Angstrom Resolution. *J. Virol.* **2007**, *81*, 4753-4765, https://doi.org/10.1128/JVI.02283-06.
54. Cheng, C.X.; Tan, M.J.A.; Chan, K.W.K.; Choy, M.M.J.; Roman, N.; Arnold, D.D.R.; Bifani, A.M.; Kong, S.Y.Z.; Bist, P.; Nath, B.K.; Swarbrick, C.M.D.; Forwood, J.K.; Vasudevan, S.G. Serotype-Specific Regulation of Dengue Virus NS5 Protein Subcellular Localization. *ACS Infect. Dis.* **2024**, *10*, 2047-2062, https://doi.org/10.1021/acsinfecdis.4c00054.
55. Venkataraman, S.; Prasad, B.V.L.S.; Selvarajan, R. RNA Dependent RNA Polymerases: Insights from Structure, Function and Evolution. *Viruses* **2018**, *10*, 76, https://doi.org/10.3390/v10020076.
56. Lee, M.F.; Wu, Y.S.; Poh, C.L. Molecular Mechanisms of Antiviral Agents against Dengue Virus. *Viruses* **2023**, *15*, 705, https://doi.org/10.3390/v15030705.

Publisher's Note & Disclaimer